Obscuring Torus in AGN as a Vortex in the Radiation Flux and its Influence on the Determined Masses of Super Massive Black Holes

V.M. Kontorovich

ABSTRACT

The influence of the radiation flux from the accretion disk on obscuring tori in active galactic nuclei and the inverse effect of torus gravity on the disk and the position of the region of broad emission lines are considered. It is shown that the latter can affect the values of masses of supermassive black holes in the centers of galaxies determined by the reverberation method.

Keywords: AGN, SMBH, obscuring (shading) torus, radiation flux, Eddington luminosity, twisting torus by radiation, streamlines (topology of), Lagrange ring, reverberation mapping.

Classification: DDC Code: 523.1 LCC Code: QB981

Language: English

London
Journals Press

LJP Copyright ID: 925642
Print ISSN: 2631-8490
Online ISSN: 2631-8504

London Journal of Research in Science: Natural and Formal

Volume 22 | Issue 10 | Compilation 1.0

Obscuring Torus in AGN as a Vortex in the Radiation Flux and its Influence on the Determined Masses of Super Massive Black Holes

V.M. Kontorovich

ABSTRACT

The influence of the radiation flux from the accretion disk on obscuring tori in active galactic nuclei and the inverse effect of torus gravity on the disk and the position of the region of broad emission lines are considered. It is shown that the latter can affect the values of masses of supermassive black holes in the centers of galaxies determined by the reverberation method.

Keywords: AGN, SMBH, obscuring (shading) torus, radiation flux, Eddington luminosity, twisting torus by radiation, streamlines (topology of), Lagrange ring, reverberation mapping.

Author: Radio Astronomy Institute NAS of Ukraine, Kharkiv.

I. INTRODUCTION. OBSCURING TORUS IN AGN

Active galactic nuclei (AGNs, see reviews [1 ,2]), responsible for the phenomenon of quasars and radio galaxies (RGs), as well as less powerful but more numerous Seyfert galaxies (Sy I and Sy II), apparently have a universal structure [3,4] and contain a supermassive black hole (SMBH, Lynden-Bell, 1969; see revs[5-7]), an accretion disk [8-9], outflowing plasma flows in the form of jets [10-12] and wind [13], and obscuring (shading) tori (ST, [3]). The latter serve as accumulators and regulators of the accreting matter and, most likely, represent grandiose self-gravitating vortices with peculiar dynamics [14]. The observed pattern of AGN depends on the orientation of the line of sight relative to the axis of the torus. When the axes are oriented close to parallel, the inner part of the AGN with broad emission lines (Sy I, quasars) is visible. If the axes are not substantially parallel and the torus obscures the central region of the nucleus, broad lines are not visible in direct radiation (Sy II, RG), but may appear in polarized light scattered by the corona [3] (see also Urry & Padovani 1995 for RGs).

It is significant that AGN together with ST represent a self-consistent system where strong gravitation, powerful radiation at a level close to the Eddington limit [15], and a peculiar vortex dynamics of ST, which is responsible for the self-consistency of the accretion and emission processes, as well as for a number of observables interacting effects in AGN. These include, in particular, bursts of radiation, correlating with emissions of superluminal components of radio jets [16].

II. ORIGIN AND PROPERTIES OF ST

The gas and dust torus is a component and result of the power accretion of matter onto the SMBH. The accretion flow itself, apparently, arises as a result of a collision or merger of galaxies [17,18]. The latter are the main reason for the emergence of massive galaxies and SMBHs at their centers [1]. Mass growth as a result of mergers formally to infinite mass is explosive [19-20] , and according to the solutions of the kinetic coagulation equation (Smoluchowski's equation) [18], is formed in a finite time. This

[1] In the Early Universe, with a deficit of heavy elements, other scenarios for the formation of massive objects are possible, related to the features of star formation under these conditions.

requires that the merger probability grows faster than the first power of the mass, which is exactly what happens in the case of gravitational interactions.[2]

The accretion disk, which is an extremely efficient converter of gravitational energy into radiation (Ya.B. Zeldovich, E. Salpeter), is formed in close proximity to the BH, starting from the boundary of stable orbits, and extends to scales of 0.01-0.1 ps [9]. The disk heats up due to the friction of neighboring layers and its thermal radiation, which is proportional to the BH mass growth rate, is limited by the Eddington limit [15], at which the radiation pressure makes it impossible for the substance to fall further onto the center. Due to the fact that the disk radiation, according to Lambert's law [21,22], is non-isotropic and mainly directed along the normal to the disk plane, where it can exceed the Eddington limit, a hollow cone free of resting matter is formed above the disk. Outside this cone, the disk radiation intensity is less than the Eddington one, as a result of which STs are formed (Fig. 1). But there is also no direct fall of matter on the center outside the cone. A torus is a (gravitational) attractor [23], around the central generatrix of which matter moves in closed orbits, forming a toroidal vortex [14]. And only a small part of this matter rotating around the toroidal attractor gets to the center and "feeds" the accretion disk [14, 24-25].

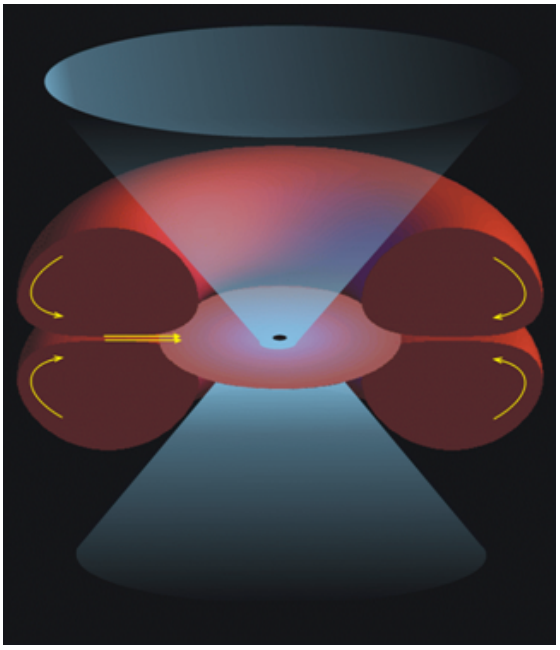

Fig.1. Diagram explaining the AGN model used. The SMBH is shown at the center of symmetry, the accretion disk in the (x-y) plane, the cone of wind and radiation from the accretion disk, the obscuring torus twisted by wind and radiation, and the streamlines inside the ST [14, Bannikova, Kontorovich, 2007].

Not shown: jets, scattering corona, accretion disk wind.

The plane of the accretion disk is a mirror plane of symmetry for the torus, resulting in a characteristic "dipole" structure of streamlines, where the "top" and "bottom" parts of the vortex rotate in opposite directions. The simplest example of such a topology can be the streamlines in the flow around a liquid cylinder [26], where the "twisting" of the substance inside the cylinder is carried out by the flow around (Fig. 2). The same topological pattern of streamlines is realized in the meridional section of the Hill vortex [27], in the Larichev-Reznik soliton [28], and other similar examples. In AGN, the corresponding "twisting" is carried out by the radiation flux from the accretion disk [14], partially "flowing around" the torus, and partially absorbed by the surface of the torus.

[2] The accelerated expansion of the Universe could put an end to this process and thus determine both the maximum mass of galaxies and the SMBH at their centers.

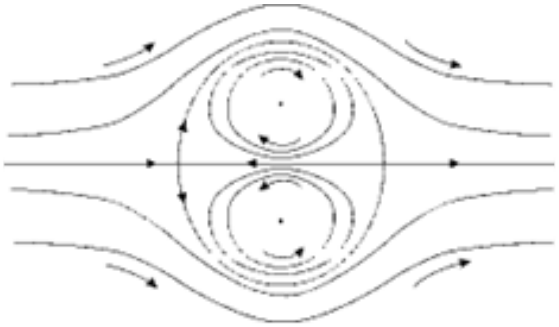

Fig.2: Topological structure of streamlines of matter and radiation similar to ones in the shading torus near AGN center: right side is the x-z section by a plane of symmetry orthogonal to the disk (left, not shown); z-axis is the axis of symmetry. The arrows show possible motions of matter in the torus and in flow around it, corresponding to the solution of the flat problem of a flow around a cylinder [14,25].

We simplify the description by replacing a small part of the torus with a large radius *R* with a circular cylinder of the same cross section with radius *a*. The angular dependence of the radiation intensity on the polar angle ϑ (with the polar axis orthogonal to the plane of the accretion disk) will be chosen in accordance with the Lambert law [22-23] in the form $I(\vartheta) = I_{\max} \cos\vartheta$. In this case, the total luminosity $L = 2 \cdot 2\pi \int_0^{\pi/2} d\vartheta \cdot I(\vartheta) = 4\pi I_{\max}$. The power of the direct radiation of the disk [3], which is not covered by the torus, is equal to $W = 4\pi \cdot \int_0^{\theta} d\vartheta \cdot I(\vartheta) = L \cdot \sin\theta$, where on the beam tangent to the surface of the torus $\vartheta = \theta$, the intensity is locally equal to the Eddington intensity: $I_{Edd} = L_{Edd} / 4\pi = I(\theta)$, $L_{Edd} \approx 1{,}5 \cdot 10^{38} M_c / M_\odot$ erg/sec. Here M_c is the mass of the SMBH and $M_\odot$ is the mass of the Sun. The foregoing requires reservations and clarifications, some of which will be explained below. The terminology used implies that the size of the disk is much smaller than the larger radius of the torus *R*, due to which the disk can be considered as a point emitter coinciding with the center of symmetry of the system, but non isotropic (according to Lambert's law) emitter.

The opening angle of the hollow cone is determined by the excess of the maximum intensity over the Eddington one:

$$\cos\theta = \frac{I_{Edd}}{I_{\max}} \quad (2.1)$$

Accordingly, with an increase in the AGN power (with some reservations), the degree of coverage of the emitting region of the ST should decrease, which, apparently, is observed according to [29] regardless of the internal structure of the torus (clamps or a continuous medium).

[3] Torus, whose temperature is much lower than the temperature of the disk, re-radiates the absorbed energy of hard radiation of the disk in the low-frequency (IR) range, which we do not take into account in these considerations. We also do not take into account the polarized radiation scattered by the AGN "corona".

III. VORTEX DYNAMICS OF AN OBSCURING TORUS

As is known [26-27, 30], the equation for the stream function ψ, $\Delta\psi = f(\psi)$, where the components of the plane flow velocity are:

$$V_x = \frac{\partial\psi}{\partial z}, \quad V_z = -\frac{\partial\psi}{\partial x}, \tag{3.1}$$

for $f(\psi) = -k^2\psi$ in polar coordinates $x = r\cdot\cos\beta$, $z = r\cdot\sin\beta$ becomes [25]:

$$\frac{\partial^2\psi}{\partial r^2} + \frac{1}{r}\frac{\partial\psi}{\partial r} + \frac{1}{r^2}\frac{\partial^2\psi}{\partial\beta^2} + k^2\psi = 0 \tag{3.2}$$

Its solution inside the circle $\psi = CJ_1(kr)\sin\beta$ at $J_1(ka) = 0$, where J_1 is the first-order Bessel function, a is the radius of the cylinder in a stream, is conjugated with the solution outside the circle $\psi = U\cdot\left(r - \frac{a^2}{r}\right)\cdot\sin\beta$, because the values of the stream function and the tangential velocity on both sides of the boundary $r = a$ coincide. This can be easily verified using the relationship of the velocity components $r\frac{d\beta}{dt} = V_\beta$, $\frac{dr}{dt} = V_r$, with the current function $\psi(r,\beta)$, which in polar coordinates takes the form:

$$V_\beta = -\frac{\partial\psi}{\partial r}, \quad V_r = \frac{1}{r}\frac{\partial\psi}{\partial\beta}. \tag{3.3}$$

It is easy to verify the latter by making the change of variables in expressions (3.1) with the help of the Jacobians

$$\frac{\partial(z,x)}{\partial(r,\beta)} = -r, \frac{\partial(\psi,x)}{\partial(z,x)} = -\frac{1}{r}\frac{\partial(\psi,x)}{\partial(r,\beta)}, \frac{\partial(\psi,z)}{\partial(x,z)} = \frac{1}{r}\frac{\partial(\psi,z)}{\partial(r,\beta)},$$

$$\frac{\partial(\psi,z)}{\partial(r,\beta)} = \frac{\partial\psi}{\partial r}\frac{\partial z}{\partial\beta} - \frac{\partial\psi}{\partial\beta}\frac{\partial z}{\partial r}, \frac{\partial(\psi,x)}{\partial(r,\beta)} = \frac{\partial\psi}{\partial r}\frac{\partial x}{\partial\beta} - \frac{\partial\psi}{\partial\beta}\frac{\partial x}{\partial r}. \tag{3.4}$$

As a result, [25] we get the value for the constant $C = \frac{2U}{kJ_1'(ka)} = -\frac{2U}{kJ_0(ka)}$, where the value $ka \approx 1,2\pi$ corresponds to the smallest root of the Bessel function J_1.

IV. RADIATION FLOW AROUND

The picture of the "flow around" the radiation flux differs significantly due to the absorption of the ST radiation and its separation on the streamline corresponding to the Eddington intensity. But inside the

torus, the topology of streamlines remains the same as in the problem of flow around a cylinder (Fig. 3).

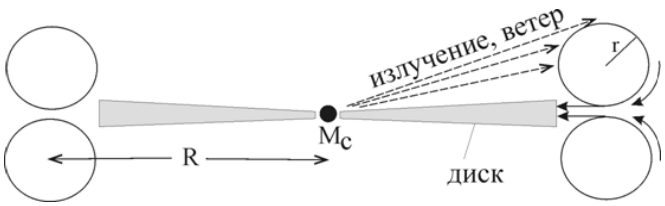

Fig.3. Scheme of "twisting" the ST by the wind and AGN radiation. External and internal critical power lines are not Shown to highlight the dipole structure torus, consisting of two counter rotating ring vortices [14,25,].

Fig. 3

The beam of field lines corresponding to the Eddington radiation intensity transmits the tangential momentum of the torus surface at the point of contact at $\vartheta = \theta$. Let us find the speed of the matter of the torus at this point, using the law of conservation of momentum, which takes the form of continuity of the momentum flux when radiation is absorbed by the shading torus. The flux density of the radiation pulse on the beam of rays of interest to us, corresponding to the Eddington intensity, is equal to

$$\frac{J(\theta)}{c} = \frac{L_{Edd}}{4\pi c\left(R^2 - a^2\right)\sin\theta} \tag{4.1}$$

Here, the distance to the point of contact of the beam is $r = \sqrt{R^2 - a^2}$, where R is the large radius of the torus - the distance to the central generatrix of the torus, counted from the center of the AGN (i.e., from the SMBH), a is the small radius of the torus.

The flux density of the tangential component of the momentum in the torus at the point of contact is [30]

$$\Pi_{tt} = \rho V_t^2 + p \,, \tag{4.2}$$

where ρ is the density of the torus, V_t is the tangential velocity, and the contribution of pressure in a relatively cold torus can be neglected.

Equating (4.1) and (4.2), we find for the tangential velocity component

$$V_t = \sqrt{\frac{L_{Edd}}{4\pi\rho c\left(R^2 - a^2\right)\sin\theta}} \tag{4.3}$$

We do not take into account the influence of the wind, but since the wind itself is a product of the radiation flux, this should not significantly affect the estimates obtained. However, the pattern of the wind streamlines near the torus should differ from rectilinear rays (Fig. 3) and, rather, will approach the pattern of flow around the material cylinder (Fig. 2). At the same time, from the condition of continuity of the tangential velocity at the point of contact of the rays $\pi - \beta = \theta$ (the equality of angles with mutually orthogonal sides was used), we find:

$$U = \sqrt{\frac{L_{Edd}}{16\pi\rho c\left(R^2 - a^2\right)\sin^3\theta}}. \qquad (4.4)$$

After that, you can use the solution formulas for the flow around the cylinder.

Thus, the radiation and the wind carry a "twist" transforming ST to a vortex. Another limiting case when the vortex is formed by initial conditions, as for example colligion or merging galaxies, see in connection of Hoag's object theory in [31].

V. INSTABILITY OF THE ACCRETION DISK PERIPHERY AND BLR IN AGN

The presence of massive STs leads to competition between two gravitational attractors: SMBH and ST. At least in the plane of the disk, this leads to the appearance of an instability region near the so-called Lagrange rings (LR) [32,33]. LR is a generalization of the interior Lagrange point for a test particle in the restricted three-body problem for the case when, along with the SMBH, the second body is a massive self-gravitating body – a torus or a massive ring. If we confine ourselves to the potential of a thin torus, it is not difficult to obtain a relationship between the mass ratio of the torus and the BH and the position of the Lagrange ring. In this consideration, we will assume that the region of broad BLR emission lines near the LR is a manifestation of the instability region. This idea is supported by the flat structure of this region observed in some cases [1, 2] and the appearance of double lines, which may be a consequence of the Keplerian rotation [4]. This representation is only an assumption [4] that needs additional observational justification. However, some conclusions that are important for the method of determining the SMBH masses by the widely used reverberation method [1, 2, 34] can follow from this.

At present, even the largest optical and IR interferometers do not have enough spatial resolution to observe (with few exceptions in the nearby Seyfert galaxies) a region of broad emission lines. But the temporal resolution turns out to be sufficient (J.Bacal) to determine the distance to the manifestation of this burst in the BLR lines [34-37] from the delay of the moment of the burst of fluctuations in the continuous spectrum of the disk emission. In this case, using the virial relations in the gravitational field of the SMBH and the measured linewidths, the BH masses at the AGN centers are determined according to $M_c = c\tau \cdot \left(\Delta V\right)^2 \cdot G^{-1}$, where the virial coefficient of the order of one-two [1,2] also appears, determined from statistical considerations. The influence of the gravitational field of the ST can significantly affect the form of this relation and, thus, the mass of the black hole determined with its help [5]. Note that for a thin torus, the position of the Lagrange Ring, near which BLR can be expected, is determined by the ratio of the masses of the SMBH and ST according to [32, 33]

$$\frac{M_c}{M_{ring}} = \frac{q}{\pi(1-q^2)}\left[(1+q)E\left(k\right) - (1-q)K\left(k\right)\right], \quad k^2 = 4q/\left(\left(1+q\right)^2 + z^2\right), \qquad (5.1)$$

[4] Another popular assumption is that BLRs are a system of clouds falling on the center or dispersed by light pressure and wind from the center encounters the difficulty consisting in the absence of an observed analogue of the shot effect.

[5] The Influence of attraction to the torus on the tangential component of the velocity near the point of tangency of the beam in this consideration can be neglected, since this force is directed approximately along the normal.

where $E(k)$ and $K(k)$ are complete elliptic integrals, k is their index, and the dimensionless lengths are measured in units of the large torus radius R.

In the general case, the virial relation for determining the mass of the SMBH should also include the mass of the ST and its geometric parameters. For a real "thick" torus of an arbitrarily smaller radius, the equation for the Lagrange ring takes the form of an integral relation, which includes the expression for the torus potential .

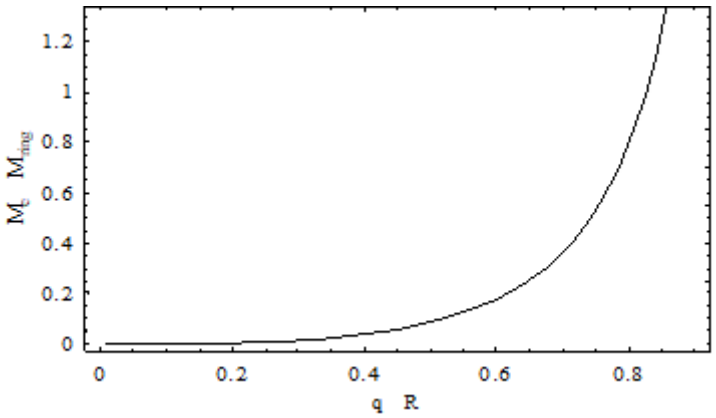

Fig.4. Dependence of the SMBH and the ST mass ratio on the relative position of the Lagrange ring q/R [33,34]

Fig. 4

If we use a convenient representation of the potential of a circular torus as a set of thin rings, it will take the form

$$\Phi(\xi,\eta) = G\int_{-a}^{+a} d\eta' \int_{-\sqrt{R^2-a^2}}^{+\sqrt{R^2-a^2}} d\xi' \cdot \rho \cdot \phi(\xi,\eta;\xi',\eta') \quad , \tag{5.2}$$

where $\xi - \eta$ are Cartesian coordinates x-z, counted from the center of the torus cross-section x-z, $\phi(\xi,\eta;\xi',\eta')$ is the potential created at a point ξ ,η by a thin ring ξ',η' of unit density (see, for example, [37-39]).

For a homogeneous torus with constant density

$$\Phi = \frac{M_{ring}}{2\pi^2 R a^2}\tilde{\Phi} \quad , \tag{5.3}$$

where $\tilde{\Phi}(x,z)$ is the specific torus potential per density unit.

The external and internal potentials of the torus were estimated in [39] using these relations. They can be used in numerical-analytical calculations of the effect of ST on the SMBH mass, determined by the reverberation method (Bacal, detailed theory developed by R.Blandford and McKee) [34-36] by the measured delay $c\tau$, which appears in the virial relation of the type (the region of instability is assumed for simplicity to lie in the plane z=0)

$$(\Delta V)^2 = \frac{GM_c}{c\tau} + \frac{M_{ring}}{2\pi^2 R a^2}\tilde{\Phi}(x - c\tau, z) \quad . \tag{5.4}$$

London Journal of Research in Science: Natural and Formal

Let us illustrate this with a simplified example, when we replace the actual (from the point of view of the influence of gravity) part of the torus by a cylinder of the same (small) radius *a*, located at a distance of a large torus radius *R* from the AGN center. In the model we will assume that the position of the Lagrange ring coincides with the inner boundary of the torus, i.e. has coordinate *(R-a)*. Then the force of attraction to the cylinder at its boundary is equal to $2\pi Ga\rho$. Equating its force of attraction to the black hole, we obtain

$$\frac{GM_c}{(R-a)^2} = 2\pi G \cdot \frac{M_{ring}}{2\pi^2 Ra}.$$

Or in our model example

$$\frac{(R-a)^2}{2\pi Ra} = \frac{M_c}{M_{ring}}, \tag{5.5}$$

whence follows

$$\frac{a}{R} = 1 + \pi\frac{M_c}{M_{ring}} - \sqrt{\left(1+\pi\frac{M_c}{M_{ring}}\right)^2 - 1}. \tag{5.6}$$

With a large mass of black holes ($\varepsilon = \pi M_c / M_{ring} >> 1$) $a/R \approx M_{ring}/2\pi M_c$; otherwise a massive obscuring torus ($\varepsilon << 1$) $a/R \approx 1-\sqrt{2\varepsilon} = 1-\sqrt{2\pi M_c / M_{ring}}$.

Thus, the position of LRs and, accordingly, the region of broad lines $c\tau$ in the reverberation method, which coincides with the region of instability near the LR (up to the distance to the stable orbits closest to the LR), is affected by a correction determined by the ratio of the masses of the ST and SMBH. Returning to the torus potential and using the virial theorem, as is done in the cited papers, we can estimate it more accurately.

Note, that the dynamical model of a clumpy torus in the gravitational field of a supermassive black hole (based on ALMA observations of the velocity field of the obscuring torus NGC1068 [42]) without taking into account the pressure of radiation of accretion disk is discussed by Bannikova, et al, in [43] in the frame of N-body simulations.

APPENDIX A. PARTICLE-TO-TORUS ATTRACTION [23]

Using the simple reasoning may show that a test particle near the inner side of a self-gravitating torus is subjected to the force attracting it to a torus. First, let us consider a thin torus which extreme case is a cylinder. In fact, the test particle will be attracted to the cylinder. This alone means that the test particle inside a torus is subjected to the force directed to this latter, or to put it more precisely – to the torus part nearest to the particle.

Let us represent a torus as a system of concentric rings. Consider the elementary case, i.e. attraction of a test particle to diametrically opposite ring areas. Select two “sectors”, with their vertices at the test particle and with a small angular span, symmetric with respect to diameter of the ring passing through the test particle. Let us consider the forces of particle attraction to the opposite arcs of a ring inside sectors. If a particle is at the center of the ring, they balance each other (Fig.Aa). When decentering the

particle (along the chosen diameter), we may see that the arc mass increases (or decreases) linearly with distance from the particle, while the force changes inversely as square of distance (Fig.Ab). Therefore, the attraction force from a "distant" arc decreases, though the arc length increases, while the force of attraction to the nearest arc increases, though the arc length decreases with the particle approaching it.

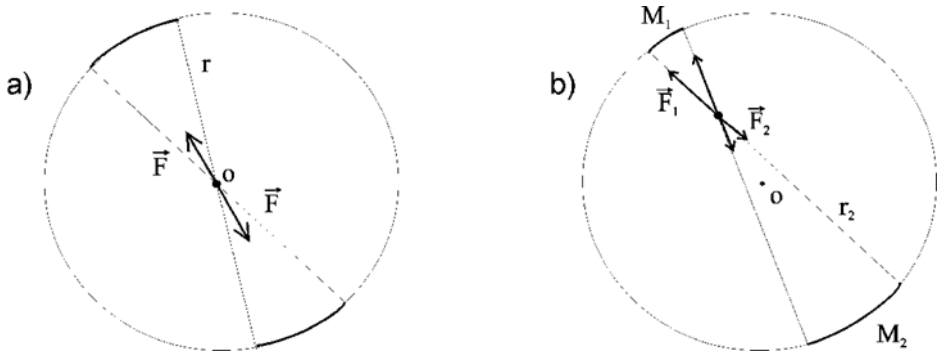

Fig. A1: Scheme of a test particle-to-ring attraction. Fragment of Fig. from the work of the BBK [23]. In the collection "Nonlinear Waves 2004"

An uncompensated force of particle-to-ring attraction and, accordingly, that of particle-to-torus appear. Expanding the span angle we are compelled to proceed from elementary formulas to integrals, though this does not change anyhow the fact of the matter and the result. It will be noted that in the case of a sphere (with the similar reasoning) the mass attracting a particle is proportional to the area on a sphere cut by a solid angle. Therefore, decentering the particle saves the exact compensation of forces: the mass is changed quadratic with the distance and is compensated by inverse dependence of the force vs. square distance. Therefore, as is notorious, a test particle inside a sphere (as against a torus) is subjected to no gravitational force.

The previous reasoning is sustained by the calculation of trajectories of test particles (Fig.A2a). Examples of trajectories for the "vertical" symmetry plane motion are shown in FigA2 [23, 44]. As can be seen from Fig.A2a and Fig. A2b, at small energies, the particle travels around a circle with minor radius, coiling around a ring (Fig.A2a shows the particle's planar motion, Fig.A2b shows the presence of orbital motion). Such motions correspond to a thin vortex (the first stage of evolution possible). With larger particle energy, different complicated trajectories appear (see, e.g. [45]).

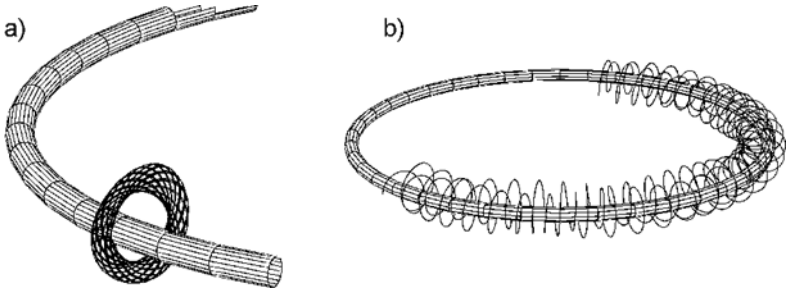

ACKNOWLEDGEMENTS

The paper was reported by Zoom in the department of theoretical physics of the Kharkiv National University seminar (chairs of E.Eserskaja and A.Zvyagin). My deep gratitude also to Voronel's and Laptev's families (especially to Vanya Laptev) for kind support from their side, Editorial of LJRS and Irina Kholodna fund for financial support, to my colleague and friend S.A. Poslavskyi for useful discussions and to Elena Bannikova for inspirationally participation in the work [14]

REFERENCE

1. Peterson BM. An Introduction to Active Galactic Nuclei,CUP: Cambridge 1997, Online ISBN: 9781139170901, 2012.
2. Netzer H. The Physics and Evolution of Active Galactic Nuclei, Cambridge, UK: CUP, 2013. AnnRevAstAp, 2015, 53: 365.
3. Antonucci R. Unified models for active galactic nuclei and quasars. ARA&A, 1993, 31: 473
4. Netzer H. Revisiting the Unified Model AGN. Annu. Rev. Astron. Astrophys. 2015, 53: 365-408.
5. Britzen S. Black Holes in a Violent Universe. New Astronomy Reviews, 2012, 56: 33–36.
6. Popovic LC. Supermassive binary black holes and emission lines in active galactic nuclei. New Astronomy Reviews, 2012, 56: 74.
7. De Rosa A et al. The quest for dual and binary supermassive black holes: A multi-messenger view. New Astronomy Reviews, 2019, 86: 101525
8. Liu BF. and Erlin Qiao. Accretion around black holes: The geometry and spectra, iScience, 2022, 25: 103544.
9. Salpeter EE. Accretion of interstellar matter by massive objects. ApJ, 1964, 140: 796–800.
10. Beskin VS. MHD Flows in Compact Astrophysical Objects: Accretion, Winds and Jets. 2009.
11. Blandford R, Meier D and Readhead A. Relativistic Jets from Active Galactic Nuclei. ARA&A, 2019, 57:467.
12. Romero GE. The content of astrophysical jets. Astronomical note, 2021, 342 (5): 727.
13. Faucher-Giguere C-A and Quataert E. The physics of galactic winds driven by active galactic nuclei. MNRAS, 2012, 425: 605–622.
14. Bannikova EYu and Kontorovich VM. A Dipole Vortex Model of Obscuring Tori in Active Galaxy Nuclei. Astronomy Reports, 2007, 51: 264.
15. Brightman M. et al,· Breaking the limit: Super-Eddington accretion onto black holes and neutron stars, Astro 2020 White Paper, 2019; arXiv:1903.06844.
16. Babadzhanyants MK. and Belokon ET. Optical manifestations of the superluminal expansion of the components of the millisecond radio structure of the 3C 345 quasar. Astrophysics, 1985, 23: 459.
17. Komberg BV. (1992). Quasars and Active Galactic Nuclei. In Kardashev NS. (ed.). Astrophysics on the Threshold of the 21st Century, 1992: 253.
18. Voloshchuk VM. Kinetic theory of coagulation, Leningrad: Gidrometeoizdat, 1984. 284 p.
19. Kontorovich VM, Kats AV and Krivitsky DS. “Explosive" evolution of galaxies in a model of coalescence events and an epoch of quasar formation. Pis'ma Zh. Eksp. Teor. Fiz. 1992, 55(1): 3-7.
20. Kontorovich VM. The evolution of galaxies in the mirror of the coagulation equation. LTP, 2016, 43: 41.
21. Born M. and Wolf E. Principles of Optics, CUP, 2013.
22. Landsberg GS, Optics. Moscow: Fizmatlit, 2003. 848 p.
23. Bannikova EYu Bliokh KYu and Kontorovich VM. Evolution and collapse of self-gravitating toroidal vortex. In: Nonlinear Waves’ 2004, Nizhniy Novgorod, 2004, 14p.
24. Bliokh KYu and Kontorovich VM. On the Evolution and Gravitational Collapse of a Toroidal Vortex. Journal of Experimental and Theoretical Physics, 2003, 96(6) : 985–992.
25. Lamb H. Hydrodynamics (Dover Books on Physics) Cambridge University Press, 1947.
26. Milne-Thomson L. Theoretical Hydrodynamics, Ed. Journal of Applied Mechanics 1968.
27. Larichev VD and Reznik GM. On two-dimensional solitary Rossby waves. Soviet Doklady, 1967, 231: 1077.
28. Kats AV and Kontorovich VM. Merger Driven Explosive Evolution of Distant Galaxies (Minor Mergers). Astrophysical Bulletin, 2013, 68: 273; astro-ph/1309.0957, 2013.
29. Mateos S, et al. Survival of the Obscuring Torus in the Most Powerful AGN. The ApJLetters, 2017, 841:L18.

30. Landau LD and Lifshitz EM. Hydrodynamics. Nauka, Moscow (1986).
31. Kontorovich VM and Poslavskyi SA. Swirling self-gravitating vortex as the imagination of the Hoag's ring galaxy, LTP, 2022, 48(5): 413-419.
32. Bannikova EYu and Kontorovich VM. Invited talk: Central mass influence on evolution of self-gravitating toroidal vortex. In: International Symposium Topical Problem of Nonlinear Wave Physics, St. Petersburg- – N.Novgorod, 2005.
33. Bannikova Elena Yu. The structure and stability of orbits in Hoag-like ring systems. MNRAS, 2018, 476: 3269–3277.
34. Gaskell M. What broad emission lines tell us about how active galactic nuclei work. New Astronomy Reviews, 2009, 53: 140.
35. Blandford RD and McKee CF. Reverberation mapping of the emission line regions of Seyfert galaxies and quasars, Astrophysical Journal, 1982, 255: 419.
36. Cackett EM, Bentz MC and Kara E. Reverberation mapping of active galactic nuclei: From X-ray corona to dusty torus, iScience, 2021, 24: 102557 .
37. Kondratyev BP. Potential Theory. New methods and problems with solutions. Moscow, Mir, 2007.
38. Batygin BB and Toptygin IN. Contemporary electrodynamics, Part 1. Moscow-Izhevsk: "R & C dynamics", 2003, 736 p. (in Russian).
39. Bannikova EYu, Vakulik VG and Shulga VM. Gravitational potential of a homogeneous circular torus: a new approach, MNRAS, 2011, 411: 557.
40. Peterson BM. The Broad-Line Region in Active Galactic Nuclei. Lect. Notes Phys. 2006, 693: 77–100.
41. Marziani P and Sulentic JW. Estimating black hole masses in quasars using broad optical and UV emission lines. New Astronomy Reviews, 2012, 56:49.
42. Garcia-Burillo S, Combes SF, Ramos Almeida C, et al. ALMA images the many faces of the NGC 1068 torus. A&A, 2019, 61: 632.
43. Bannikova E, Sergeyev A, Akerman N, Berczik P, Ishchenko M, Capaccioli M and Akhmetov V. Velocity and velocity dispersion maps for interpretation of ALMA observations. Mon. Not. R. Astron. Soc., 2021,503, Issue 1: 1459-1472.
44. Bliokh KYu and Kontorovich VM. JETP, 2003, 123: 1123 (astro-ph/0407320); 2003, Letters to Astron.J., 29, 816 (astro-ph/0409067).
45. Lavrentyev MA and Shabat BV. Problems of Hydrodynamics and their Mathematical Models. 1973, Nauka, Moscow. 416 pp. (in Russian).

This page is intentionally left blank